

# Atomistic resolution structure and dynamics of lipid bilayers in simulations and experiments

O. H. Samuli Ollila<sup>1,\*</sup>

<sup>1</sup>Aalto University

(Dated: November 2, 2015)

Recent progress in the analysis of lipid bilayer atomistic resolution structure and dynamics using combination of robust experimental data and molecular dynamics simulations is reviewed. The focus is on order parameters and spin relaxation times measured with NMR and on form factors measured with SAXS and SANS for phosphatidylcholine lipid bilayers. The experimental observables are chosen since these experiments are robust, well understood, highly reproducible and the connection between raw data and simulations is straightforward. Also the comparison between simulations and these observables is bidirectionally useful; it will quantitatively measure the quality of the simulation model respect to the reality, and if the quality is sufficient, the simulations give structural interpretation for the experimental data. Significant advance of molecular dynamics simulation models is that the same simulation model can be simultaneously compared to all of this parameters. If satisfactory agreement is found, it is highly likely that the model represents the reality due to the large amount of reproduced independent experimental parameters. In this case all the mentioned experiments would be simultaneously interpreted with the same model. Phosphatidylcholine lipids are chosen since large portion of model membrane studies have been focused on this lipid, producing enough experimental and simulation data to draw comprehensive picture on the level of understanding atomistic resolution structure and dynamics. We conclude that the acyl chain region structure and its changes are generally well described in simulations, in contrast to the glycerol backbone and choline. Also cation binding is significantly overestimated by several models.

## INTRODUCTION

**1.Samuli: Add citations to the introduction. Rewriting is also needed** Atomistic resolution molecular dynamics simulations of lipid bilayers are nowadays widely used technique to seek answer to various research questions. Typically interactions between other biological molecules (e.g. proteins, drugs, ions etc.) and lipids are studied but sometimes also lipid properties are directly under interest. The questions are often biologically motivated and the atomistic resolutions simulations gives very detailed information which is experimentally unattainable.

When simulations are used in this kind of studies, it is necessary to understand the limitations of the method and also the accuracy of the used model. In the pioneering atomistic resolution lipid bilayer simulations the quality of the simulation respect to reality was measured mainly by comparing the acyl chain order parameters and area per molecule between experiments and simulations. Especially some simulation models reproduced these amazingly well which led to the wide usage of these models.

Despite of the success of the models to reproduce the acyl chain properties and molecular density more or less correctly, already early days it was pointed out by comparing simulations to various experiments that the glycerol backbone and choline headgroup order structure may not have been correctly described. However, at the time simulations were very short compared to currently accessible timescales and it was not clear if the molecules had time to sample all the states the model would predict. Also the method to quantitatively measure atomistic resolution molecular dynamics and compare to simulations was not available, thus the real sampling timescales were not known. For these reasons the estimates of the quality of headgroup were inconclusive on the early days of molecular dynamics simulations of lipid bilayers and the

issue has gained more attention only very recently.

While the C-H bond order parameters for all hydrocarbon segments are yet the core parameter to quantify the lipid model quality, the area per molecule is quite generally replaced with form factor. The main reason is that the area per molecule is calculated from the scattering data using a model (set of assumptions). Thus, when this value is compared to the value from simulations, the simulations are not compared directly to experiments but to a value which comes from another model (set of assumptions to calculate the area per molecule). For this reason the area per molecule is nowadays replaced by comparison between form factor from simulations and x-ray or neutron scattering.

In this review we discuss the current state of the art methods to compare the atomistic resolution lipid structure and dynamics in simulations to the experiments. The C-H bond order parameters measured with NMR and form factors measured with x-ray or neutron scattering are discussed for structural comparison, and spin lattice relaxation rates for the comparison of dynamics. The main advantages of these parameters are that the experimental techniques are non-invasive, they are measured from multilamellar phase which is practically always present in simulations as well due to periodic boundary conditions and that the compared quantity (order parameter, spin lattice relaxation and form factor) is achieved from the actual experimental data in a robust way. The experimental results from these experimental techniques are also highly reproducible and the measured timescales are appropriate for the comparison to simulations. Also several other experimental parameters and techniques are used to quantify the simulation quality, however, none of these is as robust as order parameters, spin relaxation rates or form factor. The most commonly used other techniques are shortly discussed in the end of the review.

In this review we focus on phosphatidylcholine (PC) lipids

which has been in the focus of fundamental structural lipid studies for several decades now. However, there is a lot data available and the basis of our approach applies to other lipid types as well [? ].

## C-H BOND ORDER PARAMETERS AS ATOMISTIC RESOLUTION STRUCTURAL MEASURE

2.This is the first sketch of this section. It is composed from the content in the blog and from the things which came into my mind. A lot of references should be added, the text should be polished, things should be added and checked and figures should be improved. However, the main structure and idea of the section should be visible.

### Definition and properties of C-H bond order parameter

In lipid bilayer systems the order parameter of a hydrocarbon C–H vector is typically defined as

$$S_{CH} = \frac{1}{2} \langle 3 \cos^2 \theta - 1 \rangle, \quad (1)$$

where the angle brackets denote an ensemble average over the sampled conformations, and  $\theta$  is the angle between the C–H bond and the membrane normal. The numerical values of order parameters vary between  $-\frac{1}{2} < S_{CH} < +1$  depending on the sampled  $\theta$  distribution. The definition is motivated by its connection to the dipolar and quadrupolar splitting measured with  $^1\text{H}$ - $^{13}\text{C}$  and  $^2\text{H}$  NMR techniques, respectively. The functional form comes from the fundamental theory of interactions between spin systems which gives a connection between average molecules orientations and NMR measurables [1].

If the sampled distribution of  $\theta$  for a C–H bond are known, the order parameter can be straightforwardly calculated from Eq. 1. However, the sampled  $\theta$  distributions cannot be uniquely determined from the known order parameter. Thus the experimental order parameter values gives a set of conditions which structural molecular model (more specifically the C–H bond vectors of the model) has to fulfill but the experimental order parameters alone cannot be used to uniquely resolve the structure. The same applies practically to all experimental parameters used in biomolecular structure determination.

Atomistic resolution molecular dynamic simulations naturally produces the sampled structures from which the  $\theta$  distributions can be calculated and used in Eq. 1 to calculate the order parameters. The sampled structures in the simulation can be considered to be realistic only if the experimental order parameters are reproduced. If this is the case, the simulation can be then considered as an atomistic resolution interpretation of experimental order parameters. Before MD simulations were feasible for such usage, other models have been used for this interpretation [? ]. It is important to note, however, that the sampled structures which reproduce the order parameters are not necessarily the correct ones since, in principle, several structural models can produce the same order parameters. Significant advance of the MD models compared

to the traditional models is that the same MD structures can be straightforwardly compared to other experimental observables in addition to order parameters, like  $^{31}\text{P}$  chemical shift anisotropy [2],  $^{31}\text{P}$ - $^{13}\text{C}$  dipolar couplings [3] and scattering data [? ]. This will significantly reduce the possibility of getting unrealistic structures reproducing correct order parameters.

The probability for unrealistic structures with correct order parameters is further reduced by the detailed and accurate experimental data available for order parameters. Order parameters are known with high quantitative accuracy for each C-H bond present in the lipid molecule for several lipid types [? ]. The absolute values of order parameters can be measured two independent techniques by using either  $^2\text{H}$  NMR [4] or  $^1\text{H}$ - $^{13}\text{C}$  NMR [5–8] and the sign can be measured with two different  $^1\text{H}$ - $^{13}\text{C}$  NMR techniques [5, 6, 9]. It is also possible that two hydrogen bonds in the same carbon has different order parameters (*forking*) which can be detected with both  $^2\text{H}$  NMR [? ] and  $^1\text{H}$ - $^{13}\text{C}$  NMR [? ] techniques. As a result, for example for POPC lipid molecule in lipid bilayer there is ? order parameter numbers known experimentally and a structural model for this lipid should reproduce all of these. If some the order parameters are not reproduced, it is easy to detect the weak parts of the model since a single order parameter is very local quantity depending only on the position of two atoms (C-H pair). This is an advance over several other accurately measured NMR quantities, like  $^{31}\text{P}$  chemical shift anisotropy [2] and  $^{31}\text{P}$ - $^{13}\text{C}$  dipolar couplings [3] which depend on the position of several atoms, thus in the case of disagreement, it is more difficult to pinpoint the problems in the model.

### Order parameters from $^2\text{H}$ NMR experiments

The absolute values of order parameters are connected to the quadrupolar splitting  $\Delta\nu_Q$  ( $^2\text{H}$  NMR) measured in  $^2\text{H}$  NMR experiments through the equation

$$|S_{CD}| = \frac{4}{3} \frac{h}{e^2 q Q} \Delta\nu_Q, \quad (2)$$

where  $e$  is the elementary charge,  $Q$  is the deuteron quadrupole moment and  $h$  is the Planck's constant. The parameter  $q$  is related to the largest electric field gradient and in practise its value is not known; therefore the static quadrupolar coupling constant  $\frac{e^2 q Q}{h}$  is defined, and its value measured for different compounds in their solid state ( $\Delta\nu_Q$  measurement from the system where order parameter is known to be 1). In C-D order parameter measurements for lipids, it is typical to use the value measured for different alkenes,  $\frac{e^2 q Q}{h} = 170$  kHz. The relation between order parameters and quadrupolar splittings then becomes  $S_{CD} = 0.00784 \times \Delta\nu_Q$ . This relation is useful as many publications report only the quadrupolar splittings. For a review and more accurate description see the work of Seelig [4].

### Order parameters from $^{13}\text{C}$ NMR experiments

To determine order parameter with  $^1\text{H}$ - $^{13}\text{C}$  NMR experiments, the dipolar splitting  $\Delta\nu_{\text{CH}}$  is measured. This is then related to the effective dipolar coupling  $d_{\text{CH}}$  through a scaling factor depending on the pulse sequence used in the experiment [5–8]. The effective dipolar coupling  $d_{\text{CH}}$  is connected to the absolute value of order parameter through equation

$$|S_{\text{CH}}| = \left(\frac{D_{\text{max}}}{2\pi}\right)^{-1} d_{\text{CH}}, \quad (3)$$

where  $D_{\text{max}} = \frac{\hbar\mu_0\gamma_h\gamma_c}{4\pi(r_{\text{CH}}^3)}$ .  $r_{\text{CH}}$  is the C-H distance,  $\mu_0$  is the vacuum permittivity, and  $\gamma_h$  and  $\gamma_c$  are the gyromagnetic constants for  $^1\text{H}$  and  $^{13}\text{C}$  nuclei. In contrast to Eq. 2, all the parameters in Eq. 3 are in principle known. However, for the internuclear distance only the average  $r_{\text{CH}}$  is known, not the third moment  $r_{\text{CH}}^3$ . For this reason values between 20.2–22.7 kHz are used for  $\frac{D_{\text{max}}}{2\pi}$  depending on the original authors [5–8, 10? ].

### Quantitative accuracy of experimental order parameter values

It must be stressed that  $^2\text{H}$  NMR and  $^{13}\text{C}$  NMR are fully independent experiments since the deuterium quadrupolar splitting  $\Delta\nu_Q$  and the dipolar splitting  $d_{\text{CH}}$  are different physical observables. In addition, the prefactors connecting the observables to the order parameter (Eqs. 2 and 3) are independently measured. Further independent experiments are performed With  $^{13}\text{C}$  NMR by measuring the  $^1\text{H}$ - $^{13}\text{C}$  dipolar couplings using different pulse sequences [5–8] when the connection between dipolar splitting  $d_{\text{CH}}$  and effective dipolar coupling  $d_{\text{CH}}$  is different.

The measurements of quadrupole  $\Delta\nu_Q$  and dipolar  $d_{\text{CH}}$  splittings are relatively accurate, especially for quadrupolar splitting. **3.How accurate exactly?** Thus the quantitative accuracy of measured order parameters is mainly determined by the prefactors connecting the measured splittings to the order parameters (Eqs. 2 and 3). Since the prefactors are independently determined for the  $^2\text{H}$  and  $^{13}\text{C}$  NMR measurements, the quantitative accuracy is best estimated by comparing the independently measured order parameter values.

The comparisons between order parameters measured with  $^2\text{H}$  NMR and  $^{13}\text{C}$  NMR by several authors shows very good agreement [6–8, 11]. Botan et al. collected literature values for PC lipid choline headgroup and glycerol backbone order parameters and concluded that order parameters would be known with the accuracy of  $\pm 0.02$  for these segments in purified PC lipid bilayer samples [11] which agrees with the estimate of Gross et al [6]. The lower order parameter reported in some studies [5, 9, 12] were suggested to arise from lower experimental accuracy. The values collected by Botan et al. and the suggested sweet spots where choline and glycerol backbone order parameters should fall in the simulation models are shown in Fig. 1 A).

Acyl chain order parameters from different techniques are compared in Table 1 by Gross et al. [6], Dvinskikh et al. [7] and Ferreira et al. [8]. The comparison by Ferreira et al. [8] is also shown in Fig. 1 C). Generally good agreement between different methods is seen also for acyl chain order parameters, however, for some segments the 0.02 accuracy might not be achieved. **4.Maybe specify to which ones?**

### Qualitative accuracy of experimental order parameter values

When order parameters are measured as function of changing condition (e.g. temperature, hydration level, ion concentration, etc.), the prefactors connecting the order parameter and the experimentally measured couplings can be considered to be unchanged. Therefore, accuracy of the measured change is determined by the accuracy of the splitting measurement in contrast to the previous section. Here we refer to this as a qualitative accuracy. Due to the high resolution of splitting measurements, especially in  $^2\text{H}$  NMR, the qualitative accuracy is much higher than the quantitative accuracy discussed in previous section.

The high qualitative accuracy of  $^2\text{H}$  NMR experiments is exemplified in Fig. ?? by using the the classical experiment by Akutsu and Seelig [14], where the effect of different ions on the quadrupolar splittings of choline headgroup  $\alpha$  and  $\beta$  segments was measured, [86] see Fig. ??. The effects of different ions on the quadrupole splittings are clearly differentiable with the experimental accuracy in Fig. ?? A). However, when transformed to the order parameter units, these changes correspond only changes below 0.03 units for  $\beta$  and 0.05 for  $\alpha$  as shown in Fig. ?? B).

As another example of the high qualitative accuracy of order parameter experiments, the measured order parameters for  $\beta$  and  $\alpha$  carbons as a function of hydration level for different PC lipids are shown in Fig. 3. Quantitative numbers from different experiments show slight variation between different temperatures and lipid compositions. However, in all experiments the order parameters increase with decreasing hydration. [87] The smallest order parameter change is only slightly above 0.01 units, measured by Dvinskikh et al. with  $^{13}\text{C}$  NMR [31], demonstrating that high qualitative accuracy can be also achieved with  $^{13}\text{C}$  NMR.

In conclusion, the experimental qualitative accuracy order parameter measurements is very high. It is much higher than the accuracy achieved with state of the art MD simulations. Thus, the accuracy order parameter change comparison between simulations and experiments is limited by the simulation accuracy, not experimental.

On the other hand, it should be noted that since even very small splitting changes can be detected experimentally one should always connect these to the changes in real molecules to avoid overinterpretation. For example, it has been measured that cholesterol induces a measurable change in ? quadrupolar splitting which is ? [? ]. This may tempt to conclude that cholesterol affects to the choline structure, however, this

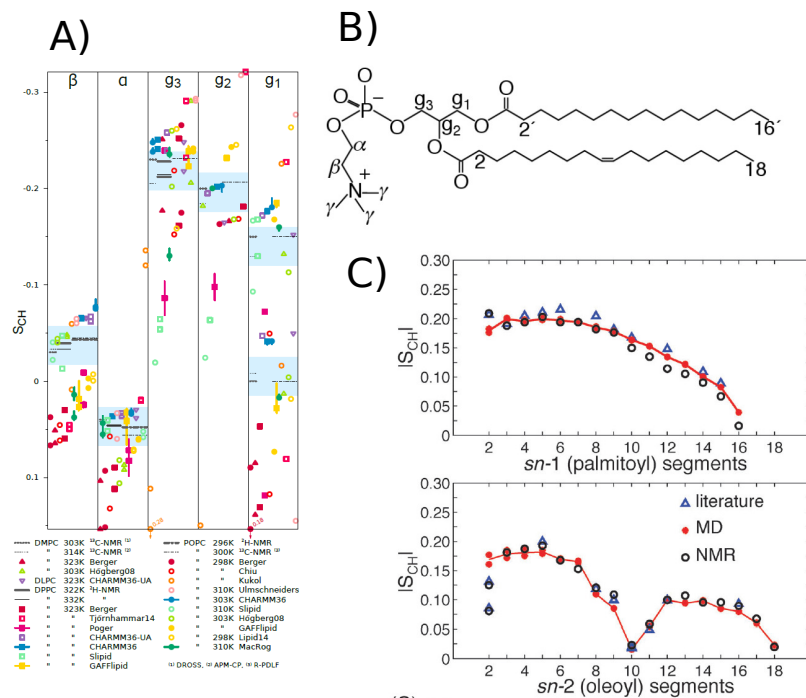


FIG. 1: A) Order parameters from simulations and experimental values from literature for glycerol and choline groups collected by Botan et al. [11]. The experimental values were taken from the following publications: DMPC 303 K from [6], DMPC 314 K from [7], DPPC 322 K from [13], DPPC 323 K from [14], POPC 296 K from [15], and POPC 300 K from [8]. The original citations for the force fields used in the simulations are Berger [16], Hogberg08 [17], Poger [18], Ulmschneiders [19], Kukol [20], Chiu [21], CHARMM36 [22], GAFFlipid [23], Slipid [24], MacRog [25], Tjörnhannmar14 [26], Lipid14 [27], CHARMM36-UA [28]. The vertical bars shown for some of the computational values are not error bars, but demonstrate that for these systems we had at least two data sets (see Table 1 in Botan et al. [11]); the ends of the bars mark the extreme values from the sets, and the dot marks their measurement-time-weighted average. The interactive version of this figure is available at <https://plot.ly/~HubertSantuz/72/lipid-force-field-comparison/>. B) Chemical structure of 1-palmitoyl-2-oleoylphosphatidylcholine (POPC). C) Picture adapted from [8]. Order parameter magnitude  $|S_{CH}|$  vs. carbon segment number for the sn-1 and sn-2 acyl chains of POPC (A and B respectively). Data from fully hydrated POPC at 300 K obtained with  $^1H^{13}C$  solid-state NMR (black dots) [8] and MD simulations (red dots) [8], as well as data from  $^2H$  NMR (blue triangles) (sn-1 [29] and sn-2 [29, 30] at 300 K).

quadrupolar splitting corresponds to unit change in the order parameter which indicates almost negligible conformational change [11].

### Signs of order parameters

While only the absolute values of order parameters are accessible with  $^2H$  NMR, two different  $^1H^{13}C$  NMR techniques allow also the measurement of the sign: first Hong et al. first measured order parameter signs for eggPC [5] and DMPC [9]; then later Gross et al. used a different NMR tech-

nique to measure signs for DMPC [6]. All the experiments report negative order parameters for almost all the segments, only  $\alpha$  and  $\gamma$  are positive.

Furthermore, the signs [5, 6, 9] and magnitudes [8, 11, 33] of choline headgroup and glycerol backbone order parameters are practically unaffected by the acyl tail contents of the bilayers. Thus, it can be fairly assumed that the order parameter signs for these segments are the same in all PC lipids in bilayer. On the other hand, the positive signs for  $g_1$ ,  $g_3$  and  $C_2$  has been reported by Aussenac et al. [34] which has led to some confusion in comparison between simulations and experiments [17]. However, these signs are not directly mea-

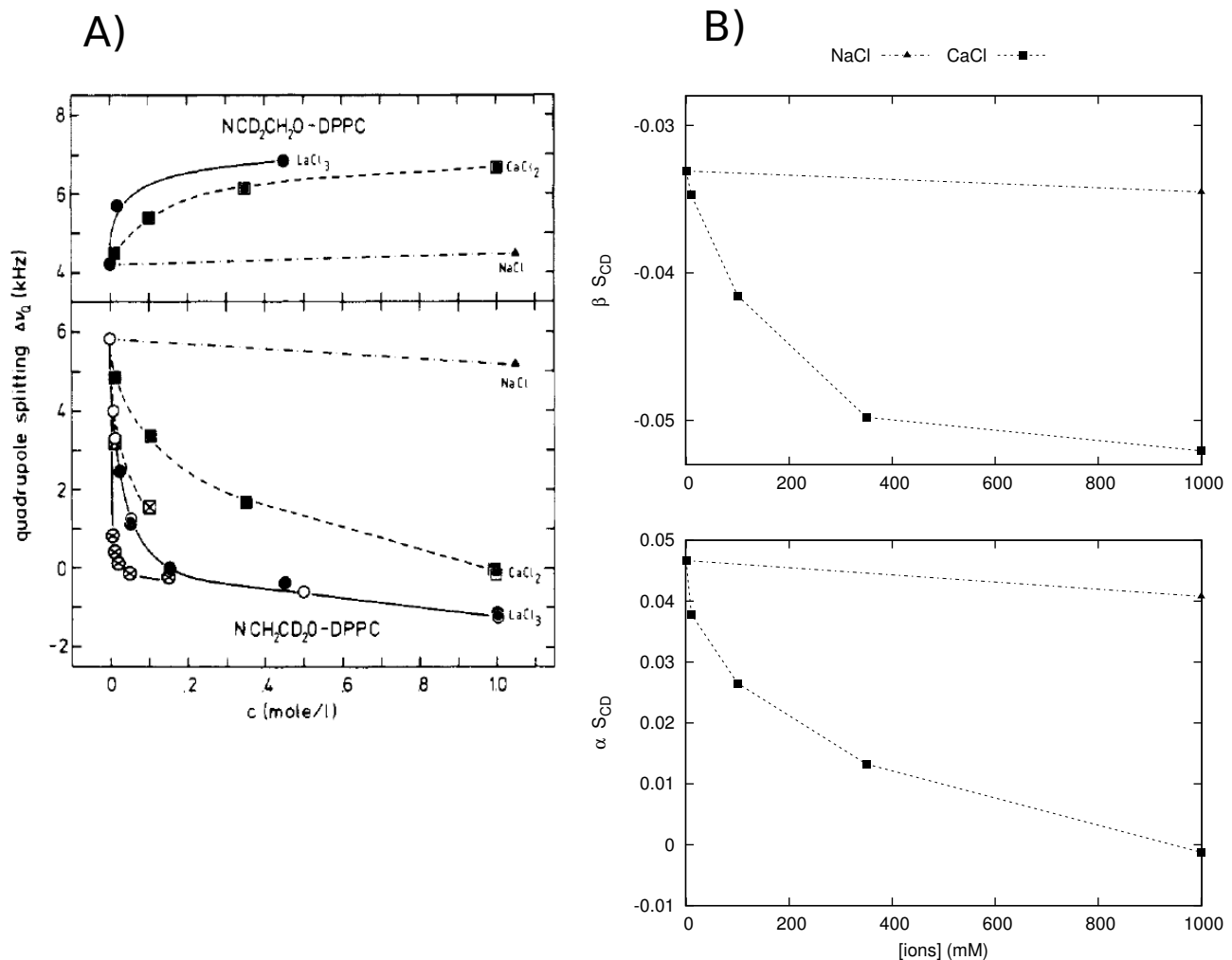


FIG. 2: A) Quadrupolar splittings as function of different ion concentrations measured by Akutsu and Seelig with  $^2\text{H}$  NMR [14]. B) The data from A) translated to order parameters ( $S_{\text{CD}} = 0.00784 \times \Delta\nu_Q$ ). Also the sign of  $\beta$  order parameter is put negative according to more recent experiments [?] (see also Ref. [11] and Section ??).

sured but extracted from the model used to interpret  $^2\text{H}$  NMR order parameters from DMPC bicelles. Thus, it is reasonable to conclude that order parameters are negative for all segments except for  $\alpha$  and  $\gamma$ , as directly measured with  $^1\text{H}$ - $^{13}\text{C}$  NMR [5, 6, 9].

Even though the sign was not measurable with  $^2\text{H}$  NMR, the sign was believed to be negative for acyl chains because  $\theta$  was expected to fluctuate around  $90^\circ$  leading to negative order parameters [4]. This was later confirmed by using  $^{13}\text{C}$  NMR measurements [5]. Also MD simulations always produce negative order parameters for acyl chains.

Typically when the response of order parameters to varying conditions (ions, dehydration and cholesterol) is measured, only the absolute values are reported [8, 14, 15, 31, 32, 35]. Where clear responses are observed, like with multivalent ions [14, 35] and dehydration [15, 31, 32], the experiments are done by gradually changing the conditions and the order parameter response is systematic, see Figs. 2 and 3. Thus, it is reasonable to assume that also the signs are not suddenly

changing. However, it seems that the sign of the  $\alpha$  carbon order parameter does change in response to a large amount of bound charge, such as multivalent ions. In this case, the absolute value of the order parameter first decreases to zero and then starts to increase again [35, 36], as seen from the nicely illustrated spectra shown Fig. 4 by Altenbach et al. [35].

### Forking of order parameters

It is possible that the  $\text{CH}_2$  segment is sampling such orientations that the order parameters for different hydrogens in the same carbon have different values. We call this phenomena as *forking*, as done also previously to avoid confusion with splittings measured with NMR. The forking is detected with both  $^2\text{H}$  NMR [29, 33, 37?] and  $^1\text{H}$ - $^{13}\text{C}$  NMR techniques [?] as two different quadrupolar or dipolar splitting values, respectively, related to the same  $\text{CH}_2$  segment.

The forking is observed for  $g_1$ ,  $g_3$ , and  $\text{C}_2$  carbon in the *sn*-



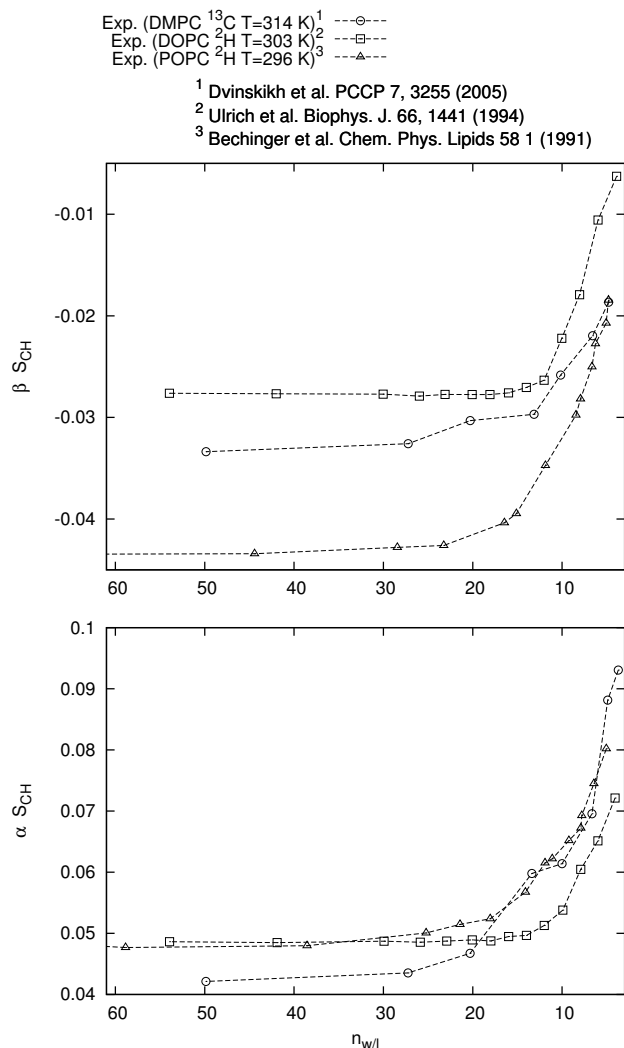


FIG. 3: Dehydration changes on  $\alpha$  and  $\beta$  order parameters measured with different methods. The data taken from Dvinskikh et al. [31], Ulrich et al. [32] and Bechinger et al. [15]. Also the sign of  $\beta$  order parameter is put negative according to more recent experiments [?] (see also Ref. [11] and Section ??).

2 chain segments in a fluid PC lipid bilayer, for other  $\text{CH}_2$  segments the equal order parameters are observed for both hydrogens are equal [8, 29, 33, 38? ?]. The forking has been studied in detail with  $^2\text{H}$  NMR techniques by separately deuterating the R or S position in  $\text{CH}_2$  segment to assign order parameters to correct hydrogens [33]. **5.Has this been done for the  $\text{C}_2$  carbon in the sn-2 chain?**

$^2\text{H}$  NMR studies also show that the forking really arises from differently sampled orientations of the two C–H bonds, not from two separate populations of lipid conformations [33, 37]. This means that realistic atomistic resolution molecular models has to reproduce the forking correctly. Thus, the simulated order parameters has to be calculated separately for each

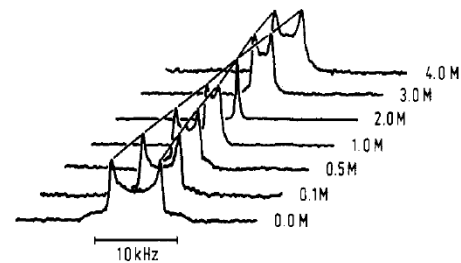


FIGURE 1:  $^2\text{H}$  NMR spectra of coarse dispersions of POPC bilayers at various  $\text{CaCl}_2$  concentrations (no NaCl). The lipid was deuterated at the  $\alpha$ -segment ( $-\text{NCH}_2\text{CD}_2\text{OP}-$ ). Measuring temperature, 40 °C.

FIG. 4: Quadrupolar splitting  $\Delta\nu_Q$  of  $\alpha$  of POPC as a function of  $\text{CaCl}_2$  concentration, related to the order parameter as  $S_{\text{CD}} = 0.00784 \times \Delta\nu_Q$ . We know nowadays that the order parameter of  $\alpha$  in the absence of  $\text{CaCl}_2$  is positive [5, 6, 9]. Thus, the most obvious interpretation for the result is that the  $\alpha$  order parameter decreases to zero when  $\text{CaCl}_2$  concentration reaches 2.0M, and above these concentrations becomes increasingly negative with further addition of  $\text{CaCl}_2$ . Reprinted with permission from Altenbach and Seelig, Biochemistry, 23, 3913 (1984). Copyright 1984 American Chemical Society.

hydrogen by taking into account the isomeric position for the structural comparison to the experimentals. Recent work by Botan et al. shows that several simulation models has problems in this respect [11] (see also Fig. ??).

### Order parameter values in the literature

For  $^2\text{H}$  NMR measurements the  $\text{CH}_2$  segments has to be labeled with deuterium. This can be done specifically for a certain segment or for the several segments simultaneously [?]. In the first case, it is known that the measured order parameter (quadrupolar splitting) is related to the labeled segment. In the latter case several order parameters (quadrupolar splittings) are measured which arise from all the labeled segments, however, it is not known which order parameter belongs to which segment. Majority of the  $^2\text{H}$  NMR data in the literature is measured from samples with perdeuterated acyl chain [39] since the synthesis of specifically deuterated lipids is complicated [?] and they are expensive. From this kind of data alone one cannot know which order parameter is assigned to which  $\text{CH}_2$  segment. On the other hand, also order parameter data from specifically deuterated lipids are available from several lipid types in various conditions [29, 33, 38? ?].

Specific labeling is not needed for order parameter measurement with  $^{13}\text{C}$  NMR due the natural abundance of  $^{13}\text{C}$ , however it could be used to enhance the signal for specific segment under interest [?]. Order parameter measurements with  $^{13}\text{C}$  NMR are 2D experiments, the chemical shift being in the first dimension and dipolar coupling in the second [?]. The chemical shift depends on the local chemical environment and is different for each carbon segment. In the sec-

ond dimension the dipolar coupling (order parameter) corresponding each chemical shift value is measured, and its value can be connected, in principle, to each carbon segment by using the chemical shift value. In practise, challenges occur in the acyl chain region where chemical shift values of different segments are very close to each others [5–8, 40]. This issue has been addressed by filtering the spectra by using partially deuterated lipids [8] and using data from simulations and specifically deuterated experiments to help in the assignment [8, 40]. It should be noted that the overlapping spectra is a challenge only for acyl chain regions with several similar segments. On the other hand, the order parameters for hydrocarbon segments in choline, glycerol backbone, close to the double bonds, and in the beginning and the end of acyl chains can be straightforwardly measured from the natural abundance lipid samples.

The order parameters are typically measured from multilamellar samples which are good for comparison to MD simulations since it is a nearest experimental correspondence for a simulation box with periodic boundary conditions. In this work we do not discuss order parameters can be measured also from other type of samples, e.g. bicelles [34, 41, 42], or indirect measurements by using, e.g. relaxation data [?] since their comparison to simulations is less straightforward.

The available experimental data for order parameters is reviewed quite recently [39, 43]. These reviews are comprehensive especially for acyl chains in pure lipid bilayer samples. In addition to this, there is significant amount of order parameter data for glycerol backbone and headgroup segments [11], and also data as a function of changing conditions for all lipid segments [7, 8, 14, 44? ]. The amount of data, especially from  $^{13}\text{C}$  NMR, has been also increasing lately [8, 40? ]. Especially the order parameter data of headgroup responses to varying conditions has a lot of unused potential since it can be used to measure, e.g. ion partitioning to lipid bilayer [14, 45? ] and lipid protein interactions [46? , 47]. Simultaneously, it gives accurate experimental parameters which can be directly compared to MD simulations [11, 45].

### Order parameters from simulations

In atomistic resolution molecular dynamics simulations molecules are sampling the defined ensemble according to the used simulation parameters and the coordinates of each atom as a function of time are saved to the trajectory files. The coordinates in the trajectory file can be straightforwardly used to calculate order parameters directly from the definition in Eq. 1. The average is taken over the molecules and time.

For simulations with united atom models without explicit hydrogen atoms [? ], the hydrogen positions can be generated post-simulationally from the positions of the heavy atoms and the known hydrocarbon geometries. This can be done explicitly by creating a trajectory with added hydrogens [11, 48], or by using equations which directly calculate order parameters from heavy atom positions [49? ]. For C–H and C–H<sub>2</sub> seg-

ments without forking these two approaches gives essentially identical results when applied correctly. However, the latter is valid only for the cases with no forking, i.e. order parameters are equal for both hydrogens attached to the same carbon. Since this is not known *a priori* for the analyzed model, it is better to use the first approach with explicitly added hydrogens.

The difference in the forking analysis is most likely reason for different choline and glycerol backbone order parameters reported in the literature for the same model [11, 50]. Also different order parameters from the same model for C–H bonds has been reported in literature [48, 51] which most likely arises from incorrect implementation of widely used version of *g\_order* program in the Gromacs package for this segment. Also, the *g\_order* program prints  $-S_{\text{CH}}$  which is most likely the reason to the reported positive order parameters for acyl chains in some studies [52]. When these issues are taken into account, the order parameters from the same models reported in the literature are generally in good agreement.

The statistical error estimates for order parameters in simulations are estimated by using the error of the mean calculated averaging over time blocks [48], over independent simulations [50] and over different lipids [11]. The maximum error bars given by all these approaches are  $\sim \pm 0.01$ .

It was recently pointed out that the sampling of individual dihedral angles might be very slow compared to the typical (100 ns) simulation timescales [53]. This result raises a question if typical simulation time scales are long enough to allow the molecules to sample the full phase space. On the other, another recent study showed that the slowest rotational autocorrelation function observed (for  $g_1$  segment) in the Berger model reached a plateau ( $S_{\text{CH}}^2$ ) after  $\sim 200$  ns and its relaxation was significantly too slow compared to NMR relaxation experiments [10]. This indicates that if the typical simulation times are too short for the full sampling of the structures, then the dynamics is unrealistically slow in the simulation model.

### Comparison between order parameters from simulations and experiments

Since the early days of lipid bilayer simulations the acyl chain order parameters are commonly calculated and compared to experiments when validating simulation studies [16, 54? –64]. Practically all the state of the art force field parametrization publications report these to be in good agreement with experiments [2, 16–28]. It is remarkable that the experimental order parameters for acyl chains in fully hydrated pure lipid bilayers can be reproduced within experimental error, see also Fig 1 C).

Exception is the C<sub>2</sub> segment in *sn*-2 chain in all PC lipids which is known to have measurable forking and lower magnitudes compared to other order parameters in the beginning of the acyl chain [? ]. This important structural fingerprint is related to the different conformations between carboxyl segments in the beginning of chains [? ]. This feature is, how-

ever, not analyzed or not reproduced for several lipid models [2, 17, 19–21, 23–26] while some models report the lower magnitude but the forking is not reproduced correctly or analyzed [2, 22, 27]. The united atom CHARMM36 is really close the experimental results [28].

In addition to the quantitatively good agreement in pure bilayers, the changes in acyl chain order parameters as a function of changing conditions are generally reasonable. For example, experimentally observed increase of order parameters as a function of cholesterol concentration [8, 49, 65, 66] and with dehydration [31, 44] are reproduced in simulations [8, 49, 67–72]. However, systematic and quantitative comparisons of these effects between experiments and simulations are rare [8, 72]. Comparison between widely used model (Berger lipids [16] and Höltje cholesterol model [73] [88]) for cholesterol containing lipid bilayer revealed that even though the acyl chain response is reasonable, the simulation model cannot be considered to agree with experiments with 34% and higher cholesterol concentrations. CHARMM36 model has been shown to slightly underestimate the cholesterol ordering effect in DMPC bilayer [70], while Slipids [71] and Lipid14 [72] models show satisfactory agreement. Lipid14 is also compared to the same extensive experimental data for POPC/cholesterol as Berge/Höltje model [8] and the agreement is significantly better [72], see Fig. 5. Also the orientation of cholesterol itself is reasonable in all models [8, 49, 70, 72], however, the cholesterol acyl chain has some issues in Höltje model [8] (too low order parameters) and in Lipid14 [72] (significant forking) while CHARMM36 reproduces experiments well [70].

The decrease of acyl chain order parameters due to the addition of double bonds is also generally reproduced by different simulation models [8, 22, 23, 27, 28, 48, 71, 74–76]. Very good agreement for oleyl chain in POPC bilayer with one *cis* double bond is demonstrated in Fig. 1 taken from Ferreira et al. [8]. Also the effect of multiple double bonds (polyunsaturation) [48, 74–76] (see Fig. 6) and difference between *cis* and *trans* double bonds can be reproduced in MD simulations [77].

In contrast to acyl chains, the order parameters for the glycerol backbone are not routinely reported in simulation literature and when reported, the agreement with experiments is concluded to be poor [11, 50, 68] or good [17, 68, 78] depending on the authors. The difference arises from different estimations for the accuracy of experimental and simulated order parameters, see also section 2. The NMRlipids collaboration recently carefully compared glycerol backbone and choline order parameters from 13 different models to the experiments and concluded that none of the available models reproduces these within experimental error, see Fig. ???. Also responses of glycerol backbone and choline order parameters to dehydration, cholesterol concentration and charge penetration were studied by the NMRlipids collaboration [11, 45]. Despite of the incorrect structures in simulation models the experimentally measured choline order parameter increase due to dehydration [11] and decrease due to penetrating ions [45] (see

Fig. 7) were qualitatively reproduced. The comparison reveals, however, that the Na<sup>+</sup> penetration is significantly overestimated by many models [45]. Also the effect of cholesterol on glycerol backbone and choline was overestimated by the Berger/Höltje model while CHARMM36 and MacRog performed better [11].

In conclusion, the experimental order parameters for acyl chains and their changes are reasonably reproduced all state of the art lipid models (except for C<sub>2</sub> segment in *sn*-2). However, all models have difficulties with varying severity to reproduce the glycerol backbone and choline order parameters, and their changes.

### Interplay between simulations and NMR order parameters: Validation and interpretation

As reviewed here, the order parameters can be measured with high accuracy for each hydrocarbon segment in lipid bilayer and the values are available in the literature for wide range of different lipids in different conditions. Thus, the experimental order parameters give very detailed and local information about the orientations sampled by each C–H bonds in the lipid bilayer system. The order parameters can be also calculated from MD simulations with high accuracy and compared to the experiments. If the order parameters agree within experimental error, the simulated structures can be considered as an structural interpretation for order parameter experiments. On the other hand, if the agreement is not good, the simulation is sampling incorrect structures.

As discussed in the previous section, the order parameters for acyl chain region from MD simulations generally agree well with experiments (except for the C<sub>2</sub> segment in the *sn*-2 chain). Thus, the acyl chain structure is most likely realistic in simulations and they can be used for structural interpretation for this region. This is a significant advancement to the traditional structural models build based on the fittings to the order parameters [? ]. The dynamical visualization of simulation trajectory immediately reveals very dynamical nature of acyl chains, rapidly sampling large amount of different conformations (for dynamics see the Section ??). These videos published by several authors in supplementary information [? ] gives significantly better intuitive understanding of dynamical nature of lipid bilayers compared to the static ones from traditional models. Since the lipid bilayers can be considered as a simplistic models for cell membranes and other biological lipid layers, this understanding has significant impact on biophysics and biochemistry.

Also the order parameter changes with changing conditions are qualitatively reproduced in the acyl chain region, however the systematic quantitative comparison of changes is rare [8, 48, 72]. The MD simulations have been especially useful to explain the origin of order parameter decrease due to *cis* double bonds in the acyl chain [48? ]. The order parameter decrease might arise from reduced order of the chain or from the changed average  $\theta$  angle in Eq. ??. From NMR



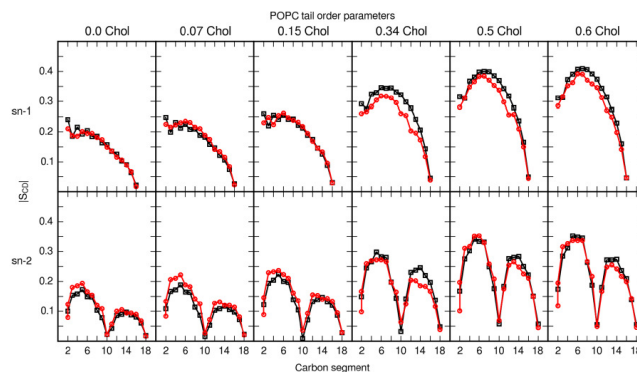


FIG. 5: Cholesterol effect on acyl chain order parameters compared between ? model [72] and experiments [8]. The agreement with experiments with this model is significantly better than Berger/Höltje based model compared by Ferreira et al. [8].

experiments alone it was impossible to judge which is the correct explanation for the decreased order parameters due double bonds [? ]. Several simulation studies by different authors using different models has showed that the decreased order parameter order parameter due to *cis* double bonds can be reproduced by introducing proper dihedral potentials next to double bonds, and due to the flexibility of these dihedrals the polyunsaturated acyl chain becomes more flexible and the order is reduced [? ]. These studies concluded that order parameter decrease due to double bonds arises from genuine disorder of the chain, not from the changes in average angle [? ]. This is a prime example of the case where MD simulations have significant advance over more traditional modeling approaches [? ].

The increase of acyl chain order parameters and related bilayer thickening due to addition of cholesterol is also qualitatively reproduced by simulations giving also intuitive visualizations for these effects [8, 72? ]. However, quantitative comparison reviewed in previous section reveals that some models do not reproduce the acyl chain order parameters within experimental error in cholesterol mixtures [8, 70]. This indicates that these models are not yet accurate enough to give atomistic resolution interpretation to delicate lipid cholesterol interactions which are known to induce liquid-ordered and liquid-disordered phase coexistence [? ]. The recent Amber model [72] seems promising in this respect, see also Fig. 5. Careful quantitative comparison of dehydration induced ordering effect has not been made but it is mentioned to be weaker in simulations compared to experiments [68]. Thus it is not clear if current simulations can be used to interpret atomistic resolution acyl chain ordering due to dehydration which has been suggested to play an important role in hydration repulsion [? ].

Simulation studies have also predicted changes in the acyl chain region which are yet to be experimentally confirmed, e.g. order parameter decrease due to lipid oxidation and changes in order parameter sign in oxidized acyl chain [52].

As discussed in the previous section, simulations models are not able to reproduce the glycerol backbone and choline

headgroup order parameters within experimental error [11] in contrast to acyl chains. Thus, even the state of the art simulation models are not able to resolve the sampled atomistic resolution structure of these segments which has been also tremendous challenge to the more traditional models [? ]. Consequently, the conclusions made from MD simulations which depend on atomistic resolution structure of energetics of these segments should be taken with extreme caution. On the other hand, the qualitative response of choline  $\alpha$  and  $\beta$  order parameters to the dehydration and penetrating ions (increase and decrease, respectively) was correctly reproduced by several models, despite of the incorrect structure in fully hydrated lipid bilayer [11, 45]. These changes could be related with the changes of P-N vector angle respect to the membrane normal as suggested previously in [? ]: the tilting of P-N vector more parallel to membrane plane with dehydration leads to the increase of choline order parameters [11] and *vice versa* with penetrating ions [45]. **6.The analysis with ions not actually done yet!** The widely used Berger/Hiltje model significantly overestimates the structural effects due to cholesterol in the glycerol backbone and choline regions [8, 11] which seems to be the case also for Lipid14 [72].

The recent progress in the NMRlipids collaboration has shown that simulations confirm the electrometer concept suggested by Seelig et al. in a serie of classical publications [? ]: the decrease of  $\alpha$  and  $\beta$  order parameters is a measure of charge penetrated in PC lipid bilayer [45], see also Fig. ???. The concept gives a direct and quantitative route to compare charge binding into PC lipid bilayers between simulations and experiments through the choline order parameters [45]. While experimental results show only very weak or negligible  $\text{Na}^+$  binding, some simulation models predict significantly stronger binding, see [45] and Fig. ??. This is a serious artefact since specific cation binding makes a lipid bilayer positively charged, which has a potential to lead incorrect conclusion when interactions with charged objects are studied. Thus the numerous conclusions from simulation studies with strongly binding  $\text{Na}^+$  has to be taken with extreme caution. In contrast to monovalent ions the  $\text{Ca}^{2+}$  and other multivalent

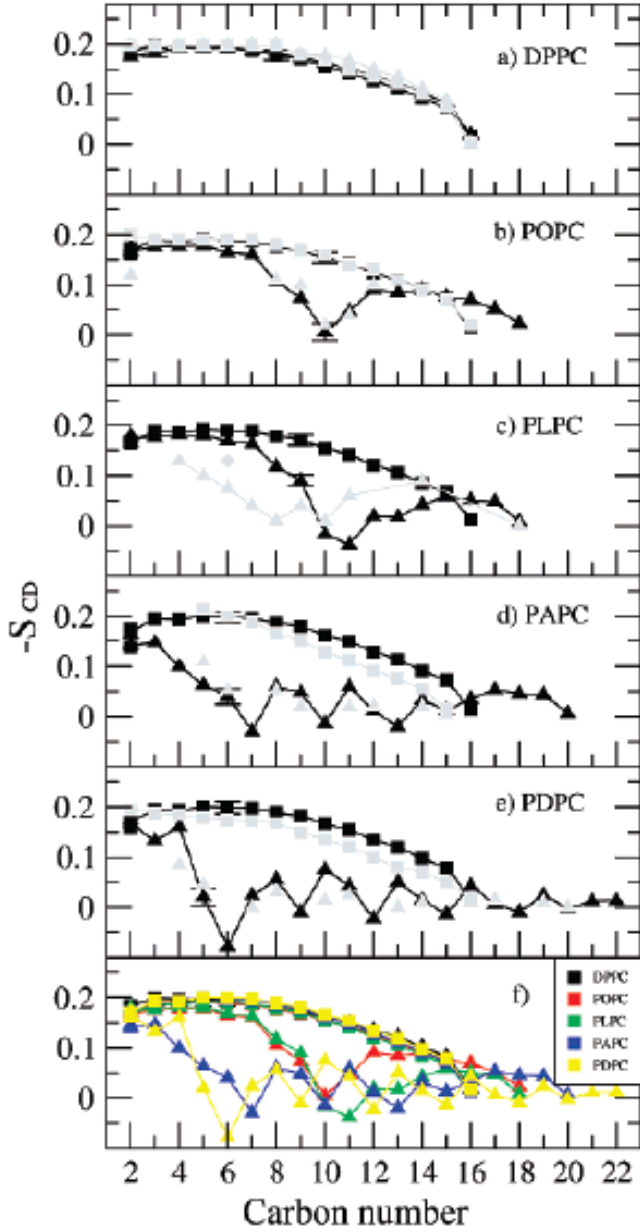


FIG. 6: Figure comparing order parameters in polyunsaturated acyl chains between simulations and experiments taken from [48]. Order parameters for the sn-1 (squares) and sn-2 (triangles) chains of (A) DPPC, (B) POPC, (C) PLPC, (D) PAPC, and (E) PDPC. Simulation results are shown in full black, and experimental results for comparison in gray. Additionally, part F summarizes the data for all bilayers from the simulations. Experimental order parameters were chosen for comparison as follows. The order parameters for DPPC (T=323K) are based on studies by Petrache et al. [?] whereas the experimental  $S_{CD}$  values for PDPC and for the sn-1 chain of POPC (T=310 K) are based on studies by Huber et al. [?] For the sn-1 chain of PDPC, the data set at 310 K is obtained by linearly interpolating between data at 303 and 323 K, whereas for the sn-2 chain the data at 303 K are presented [?]. Experimental values for the sn-2 chain of POPC are based on studies by Seelig et al. [?] A single experimental value is available also for the sn-2 chain of the PLPC bilayer at 313 K (diamond) [?] to compare with our simulated order parameters for PLPC. Together with PLPC, there are also experimental results for PiLPC (T=313K) [?]. Experimental order parameters for the sn-1 and sn-2 chains of PAPC (T=303 K) are based on quadrupole splittings measured by Rajamoorthi et al. [?]. For the sn-1 chain the monotonic decrease through the acyl chain is expected. For the sn-2 chain, values are fitted such that the agreement is as good as possible.

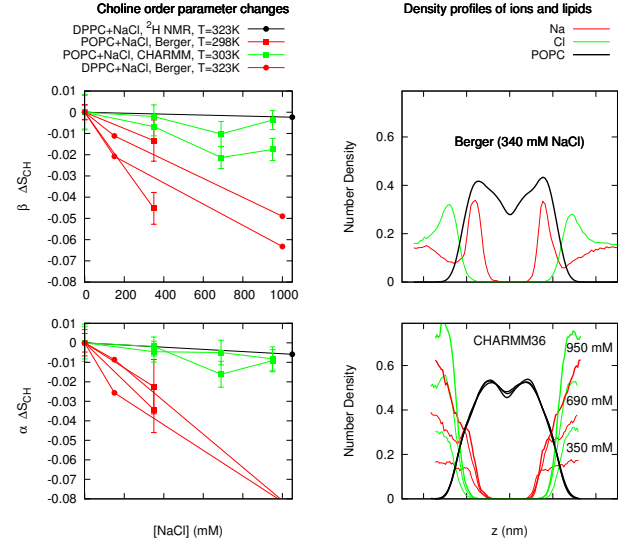


FIG. 7: Changes in order parameters as a function of Na<sup>+</sup> concentration (left column) and ion density distributions (right column). With Berger model significant order parameter reduction and ion partition is observed while with CHARMM36 modest order parameter change and ion partition observed. The results confirm the concept by Seelig et al. which allows the ion partition to be measured by changes in  $\alpha$  and  $\beta$  order parameters. The results clearly show that Berger model has too strong Na partition. For more discussion see [45].

ions significantly partition to PC bilayers [?]. This is also seen in simulations, however, the structural effects are overestimated at least in the Berger model [45]. The CHARMM36 behaves more realistically, however, more careful simulation studies are needed to conclude if some of the existing models are capable to correctly reproduce PC ion interactions [45].

In conclusion, the atomistic resolution MD simulations are invaluable in understanding the structural details and their changes in acyl chain region, especially for double bonds. However, serious artefacts are possible, or even likely, in simulations studies where choline or glycerol backbone structure, or cation binding are important.

## C-H BOND ROTATIONAL DYNAMICS FROM SPIN RELAXATION RATES AND SIMULATIONS

### Here will be described:

- How the rotational dynamics measured by using NMR relaxation experiments.
- How the relaxation experiments are connected and compared with simulations.
- What can be learned and what has been learned about the rotational dynamics from the comparison between spin relaxation and simulations

7. This is quite straightforward to write for me and there is quite good support from our recent work [10]. I will write the first version as soon as I can.

### Definition and properties of rotational autocorrelation function

The second order auto-correlation function for the reorientation of the C–H chemical bond axis is defined as [79]

$$g(\tau) = \langle P_2[\vec{\mu}(t) \cdot \vec{\mu}(t + \tau)] \rangle, \quad (4)$$

where  $P_2$  denotes the second Legendre polynomial,  $P_2(\xi) = 1/2(3\xi^2 - 1)$ ,  $\vec{\mu}(t)$  is the unitary vector having the direction of the C–H bond at time  $t$ , and the angular brackets denote a time-average. This autocorrelation is usually chosen to describe the C–H bond rotational dynamics since it is connected to the experimentally measurable spin relaxation rates through its Fourier transformation called spectral density

$$j(\omega) = 2 \int_0^\infty \cos(\omega\tau) g(\tau) d\tau. \quad (5)$$

In this review we focus only on experiments measured from multilamellar samples with randomly oriented sheets, thus only the second order auto-correlation function is needed [?].

In randomly oriented multilamellar samples the auto-correlation function of bond orientations always decays to zero with long enough time scales. However, the relaxation timescales can be divided to two distinct timescales. First the relaxation processes shorter than microsecond timescales occurs when lipid molecules are reorienting in the lipid bilayer but are not essentially moving between lipid bilayer regions with different orientations. Then with larger than microsecond timescales the movement between differently oriented bilayer regions decays the rotational correlation function to zero. In addition, MAS experiments the sample spinning causes lead orientational relaxation in kHz region. The full auto-correlation decaying to zero is illustrated in Fig. 8. Due to the timescale separation the correlation function can be written as [80]

$$g(\tau) = g_f(\tau)g_s(\tau); \quad (6)$$

$g_f(\tau)$  describes the decay of  $g(\tau)$  due to fast molecular motions and  $g_s(\tau)$  contains the contribution from slower motions

$$g_s(\tau) = e^{-\frac{\tau}{\tau_s}} \left[ \frac{2}{3} \cos(\omega_R \tau) + \frac{1}{3} \cos(2\omega_R \tau) \right], \quad (7)$$

where  $\tau_s$  is a correlation time due to slower isotropic molecular motions originating from the diffusion between bilayers with different orientations of their principal symmetry axis, and the cosine terms are the contribution from magic angle spinning of the sample, rotating at  $\omega_R/2\pi$  cycles per second [?], typically in the kHz frequency range.

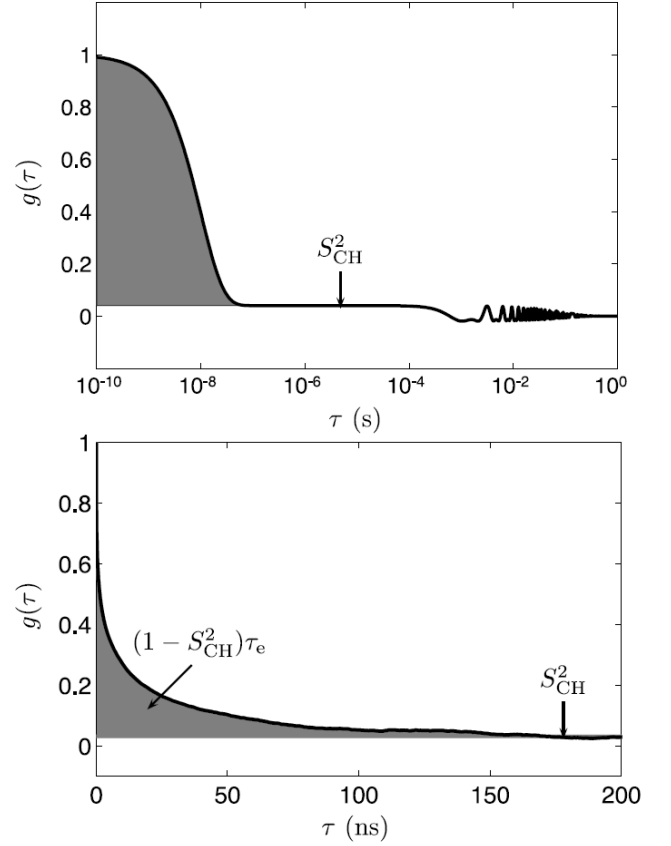


FIG. 8: (Top) Illustration of the auto-correlation function  $g(\tau)$  and effective correlation time  $\tau_e$  for a  $^{13}\text{CH}$  bond in a lipid bilayer in MAS experiment (x-axis with logarithmic scale). Plateau after short timescale relaxation processes ( $g(\tau)_f$ ) is shown between roughly  $10^{-7}$  s and  $10^{-4}$  s. After this timescale the slow relaxation processes ( $g(\tau)_s$ ) and oscillation due to MAS (Eq. ??) are shown. (Bottom) Example of  $g(\tau)$  from a united-atom MD simulation of a POPC bilayer in excess water, illustrating the decay towards  $S_{CH}^2$  (x-axis with linear scale). This represents the  $g(\tau)_f$  in Eq. ?? and decrease to the plateau in the top figure. The effective correlation time  $\tau_e$  is equal to the area in gray scaled by  $(1 - S_{CH}^2)^{-1}$ . Figure adapted from [10]

The order parameter measurements with  $^2\text{H}$  NMR and  $^{13}\text{C}$  NMR measure the bond order after the relaxation of rotational motion inside the bilayer plane but before the relaxation between different bilayer orientations, as illustrated in Fig. 8. In typical molecular dynamics simulations with periodic boundary conditions the lipid molecules are restricted to single bilayer orientation and also the timescales are currently typically below microsecond. In these simulations the auto-correlation function in Eq. 4 decays to the square of order parameter in Fig. 1 in bilayers with planar symmetry, i.e. no microscopic phase separation of defects present. Also this is illustrated in Fig. 8.

The rotational correlation function describes how long does it take for a single molecule on average to sample the confor-

mations. The effective correlation time

$$\tau_e := \int_0^\infty \frac{g_f(\tau) - S_{CH}^2}{1 - S_{CH}^2} d\tau \quad (8)$$

can be used as an intuitively useful single parameter to describe this time. The larger this parameter is, the longer it takes in average to sample the conformations related to the bond. With this definition the area between the correlation function and its plateau becomes  $(1 - S_{CH}^2)\tau_e$ .

### Detecting C–H bond dynamics experimentally

The most used parameter to detect the C–H bond dynamics experimentally in time scales comparable to simulations are the spin-lattice relaxation rates  $R_1$  from deuterium labels and  $^{13}\text{C}$ .  $R_1^C$  measured from  $^{13}\text{C}$  is connected to the spectral density (Eq. 5) through the equation

$$R_1^C = \frac{D_{\max}^2 N_H}{20} \left[ j(\omega_H - \omega_C) + 3j(\omega_C) + 6j(\omega_C + \omega_H) \right], \quad (9)$$

where  $\omega_C$  and  $\omega_H$  are the Larmor angular frequencies of  $^{13}\text{C}$  and  $^1\text{H}$  respectively,  $N_H$  is the number of bound protons and  $\frac{D_{\max}}{2\pi} \approx 22$  kHz as in section ???.  $R_1^D$  measured from  $^2\text{H}$  is connected to the spectral density (Eq. 5) through the equation

$$R_1^D = \frac{12\pi^2}{40} \left( \frac{e^2 q Q}{h} \right)^2 \left[ j(\omega_D) + 4j(2\omega_D) \right], \quad (10)$$

where  $\frac{e^2 q Q}{h} = 170$  kHz as in the case of order parameters in section ??.

Also the model free approach to measure the effective correlation time (Eq. 8) was recently introduced [10]. The method is based on the combination of experimental order parameter  $S_{CH}$ , spin-lattice relaxation rates  $R_1$  and the transverse magnetization under a spin lock pulse  $R_{1\rho}$  with measured appropriate nutation frequency.

### Analyzing C–H bond dynamics from simulations

As in the case of order parameters, the auto-correlation function for each C–H bond can be calculated directly from simulations using the definition in Eq. ?? since the trajectories of each atom is known as a function of time. As in the case of order parameters the positions of hydrogens can be determined for united atom models based on heavy atom positions and assuming tetrahedral configurations [? ]. Usually in the correlation function calculation all the available time intervals from the simulation data are used and the average over those and all molecules is taken. However, since the amount of data decreases when the the time interval approaches the total length of the simulation, usually the largest time interval used is the half of the total simulation length, for more details see [? ].

To connect the auto-correlation functions from simulations to the experimentally measurable spin lattice relaxation times, the spectral density (Eq. 5) must be first calculated. In principle, this could be done using numerical fourier transformations techniques, however this often leads to unnecessarily large fluctuations. Instead, commonly used approach is to fit analytical functional form to the calculated auto-correlation function and then use analytical Fourier transform of the fitted function [? ]. Most commonly the sum of ? or more exponentials is used as a fitting function [? ] but also stretched exponential has been used [? ]. Numerically the functional form of the fitting function should not matter as long as the fit is good, however, theoretically the correct correlation function form to describe the modes of physical motion can be debated [? ]. It is clear from correlation functions from simulations that one exponential is not enough to produce a good fit while ? gives a reasonable fit [? ]. This is not surprising since more than one relaxation timescale is definitiely expected to be present in lipids in bilayer.

After the fitting the analytical form of the spectral density predicted by simulations is available. Then its values can be calculated at the required larmor frequency values and substituted to Eqs. 9 and 10 to get the  $R_1^C$  and  $R_1^D$ . The value of the effective correlation time can be calculated directly from the iterated area below the correlation function, see Fig. 8 or from Eq. ??.

### Comparing C–H bond dynamics between simulations and NMR experiments

The spin lattice relaxation parameters  $R_1^C$ ,  $R_1^D$  and  $R_{1\rho}$  are considered as directly measurable experimental parameters and the effective correlation time  $\tau_e$  can be derived directly from directly measurable parameters without further assumptions (see Eq. ?? and Ref. [10]). Spin lattice relaxation parameters  $R_1^C$  and  $R_1^D$  can be calculated from simulations by first calculating the auto-correlation function (Eq. ??), then calculating the spectral density from the Fourier transformation (Eq. ??) and finally substituting its values into Eqs. ?? and ?? (see also previous section). The effective correlation time can be calculated directly from integrated area and order parameter or from Eq. ??. In practise, the  $R_{1\rho}$  cannot be calculated from simulations directly since its value depends also on the slow relaxation dynamics ( $g_s(t)$  in Eqs. ??) which is not present in simulations. The same applies to the calculation of NOE relaxations rates and in this case decay time of ?ns was assumed for the  $g_s(t)$ , while 4.2 ms was measured by Ferreira et al. [10].

As seen from Eqs. ??, the numerical values of  $R_1^C$  and  $R_1^D$  depend also on the carbon  $\omega_C$ , hydrogen  $\omega_H$  and deuterium  $\omega_D$  Larmor frequencies which, in turn, depend on the spectrometer external magnetic field. From simulations it is straightforward to calculate the spectral density with any Larmor frequency value to get the  $R_1^C$  and  $R_1^D$  as a function of external magnetic field, as shown in Fig. ??. However, in ex-

periments with standard spectrometers the external field cannot be changed, i.e. each spectrometer has their specific field strengths. Thus, to measure  $R_1^C$  or  $R_1^D$  values as a function of magnetic field one has to use several spectrometers which is tedious and spectrometers exist only with limited amount of magnetic field strengths. Despite of these challenges this kind of experiments have been done and the available data is reviewed by Leftin et al. [39]. Another approach to measure the magnetic field strength dependence of spin lattice relaxation times is the Field Cycling NMR [? ? ]. However, this is not yet feasible with standard spectrometer and only limited amount of data is available, mostly from  $^{31}\text{P}$  NMR [81? ? ] but also from  $^{13}\text{C}$  NMR [? ].

Few studies have compared the magnetic field strength dependence of spin relaxation times between simulations and experiments [82? –84]. Examples of such comparison for acyl chain segments are shown in Fig. 9. On the other, several studies compared  $R_1^C$  and  $R_1^D$  measured with one magnetic field strength to the value calculated from simulations [? ]. Example of such comparison between  $R_1^C$  from simulations and experiments is shown in Fig. 10. Comparisons seem to generally show a good agreement with large Larmor frequencies which is getting worse when the Larmor frequency decreases. On the other hand, the level of the agreement depends on the carbon segment and the type of relaxation used in the comparison; Berger model compared with  $^2\text{H}$  NMR gives better agreement for  $\text{C}_7$  segment compared to  $\text{C}_3$  (Fig. 9 B)) while comparison to  $^{13}\text{C}$  NMR relaxation with one frequency gives similar discrepancy for both segments (Fig. 10). For CHARMM the agreement seems better when going towards bilayer center, see Fig. 9 A). Due to the complicated connection between molecular dynamics and spin relaxation it is not straightforward to make conclusions about the dynamical differences between reality and simulations. This is, however, possible with careful analysis as discussed in the next section.

To ease the intuitive interpretation of experimentally measured rotational dynamics Ferreira et al. showed that the effective correlation time can be measured by combining directly measurable quantities [10]. It should be noted that a quantity called by authors as effective correlation or  $\tau_e$  has been reported also previously in the literature, however, these studies typically assume correlation function to have a single exponential form [? ]. Since molecular dynamical simulations and theoretical understanding indicate that assuming a single exponential decay is not realistic, the effective correlation times measured with this assumption should not be quantitatively compared to MD simulations where multiexponential decay has been observed. The approach by Ferreira et al. is model free in the sense that nothing is assumed about the short timescale correlation processes when  $\tau_e$  is measured [10]. The comparison of effective correlation times between experiments and simulations for different segments is shown in Fig. 10. From this result it is straightforward to conclude that acyl chain rotational dynamics is generally well described while in the interfacial region, especially in glycerol backbone, the dynamics is too slow in simulations. It should be

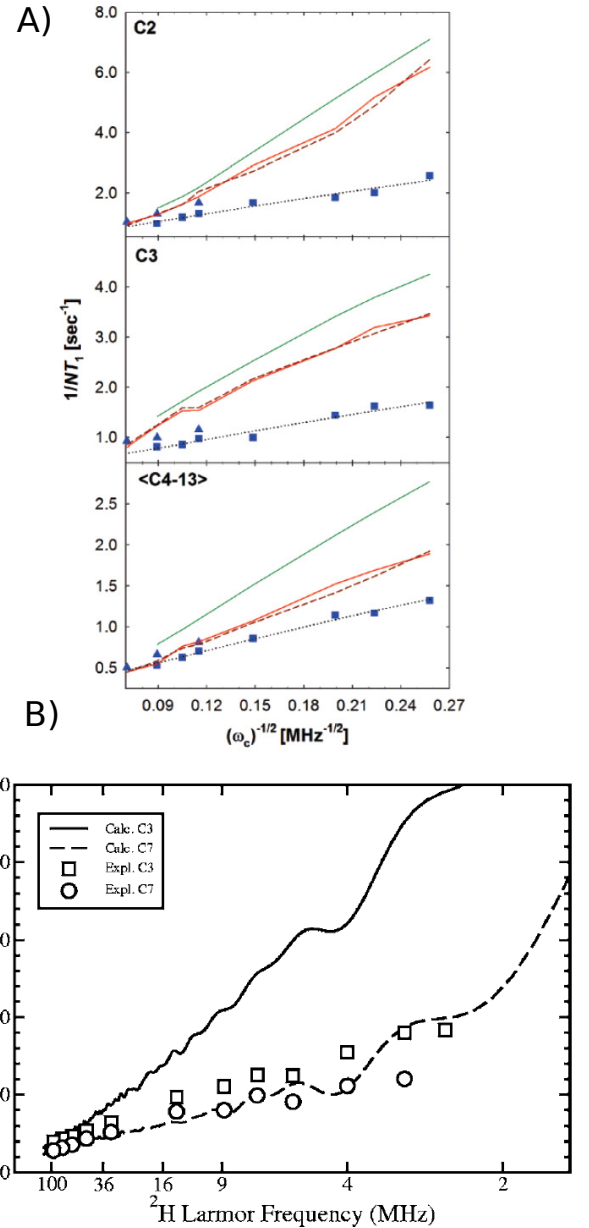


FIG. 9: A) Comparison of  $R_1^C$  dependence on magnetic field between experiments and CHARMM simulations for acyl chain carbons (DPPC bilayer in 323K) adapted from [? ]. Experiments as points; MD simulations as solid and dashed lines; and a model-free fit to the vesicle data as dotted lines. B) Comparison of  $R_1^D$  dependence on magnetic field between experiments and Berger simulations for acyl chain carbons (DMPC bilayer in 300K) adapted from [84].

noted, however, that the effective correlation describes the total relaxation over all short timescales present in  $g_f(t)$ . Even if this is correct, the balance between different processes with different relaxation times may not be correct. This is actually seen in the acyl chains, where  $R_1$  does not perfectly agree with experiments while  $\tau_e$  does.



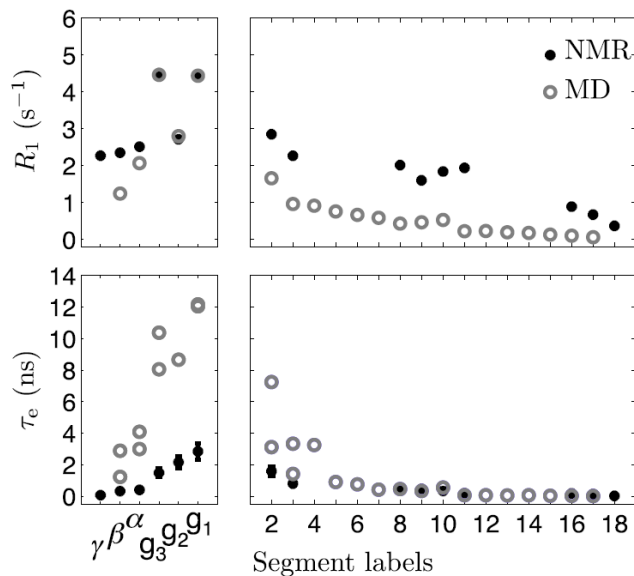


FIG. 10: (top)  $R_1^C$  for POPC bilayer in 298K calculated from simulations with Berger model compared to experimental results measured with field strength corresponding to the Larmor frequency of 125 MHz for  $^{13}\text{C}$ . (bottom) Effective correlation times for the same system compared between simulations and experiments. Figure adapted from Ferreira et al. [10].

#### Interplay between simulations and NMR spin lattice relaxation times: Validation and interpretation of dynamics

are connected to the actual molecular dynamics through the spectral density (Eq. 5) which is the Fourier transformation of the auto-correlation function 4. The spin lattice relaxation rates depends spectral density values only with certain larmor frequencies as seen from Eqs. 9 and 10. In experiments the Larmor frequency depends on the external magnetic field of the used spectrometer. Thus, with a regular NMR spectrometer only a single  $\rho$  and  $\sigma$  values can be measured. These will only give information about the size of the spectral density close to the used Larmor frequencies. However, to detect the whole rotational correlation function one should have information with all relevant larmor frequency values. The single spin lattice relaxation rates only give an estimate how much of the dynamical processes are present with the timescales roughly with inverse of Larmor frequency. Even the qualitative changes in dynamics are difficult to detect by measuring single relaxation rate values since the increase (decrease) of the value only indicates the increase (decrease) of relative significance of the relaxation with the detected timescales. If the general dynamics gets slower or faster depends what happens to the significance of relaxation processes with faster and slower timescales which are not detected by measuring single relaxation rates.

Several experimental and theoretical approaches has been use to address this issue. Temperature dependence of spin

relaxation rates have been measured to analyze the relative molecular rotational relaxation. Spectrometers with different magnetic field strengths have been used to measure points with several Larmor frequencies. Models are fitted to the spin relaxation data. The effective correlation time is measured which gives a quantitative measure of the general rotational dynamics. Also MD simulations have been successful in interpretation of the measurements of the effect of double bonds on molecular dynamics.

Comparison between spin lattice relaxation rates measured with NMR and calculated from MD is also used to validate the correctness of the dynamics in the simulations. The comparison in the early simulations revealed that there are dynamical time scales present in simulations are realistic [?]. Later on the comparison between simulations and dispersion data indicated that the simulation dynamics more or less agrees with experiments for some carbons while there is room for improvement for others [?]. However, due to the complicated connection between spin lattice relaxation rates and molecular dynamics it is difficult to conclude from these comparison if the dynamics is too slow or fast in the simulations. This issue can be clarified by measuring the effective correlation times with recently introduced methods [10]. The comparison between effective correlation times from experiments and simulations reveals that the rotational correlation dynamics is too slow for the glycerol backbone and choline in Berger model. However, this is not very surprising since the Berger model is also sampling wrong configurations for these segments. However, the experimental data and similar comparison would be useful for models sampling more realistic structures, e.g. CHARMM36 which dynamics do not fully satisfy the dispersion data.



## STRUCTURE FACTORS FROM SCATTERING AND SIMULATIONS

**For this section I would be more than happy for some help**

**Here will be described:**

How are the form factors are measured.  
What is the primary experimental observable.

**On these questions I do not know the answer and it is not exactly clear from where I can find the answers. More specifically:**

**8. Which is the experimental quantity that the scattering machinery exactly puts out?**

**How the form factor is determined from the experimental observables?**

**Which assumptions are needed here?**

**There is already some discussion about this in the blog by Peter Heftberger and Georg Pabst, but any kind of information from full explanation with citations to the hints of relevant literature are helpful here. The more detailed discussion can be found at:** <https://github.com/NMRLipids/NMRLipids-V-Review/issues/1>

How accurate are the experimental form factors.

**9. Has this been discussed in the literature already? Any kind of information from full explanation with citations to the hints of relevant literature are helpful here. The more detailed discussion can be found at:** <https://github.com/NMRLipids/NMRLipids-V-Review/issues/2>

How the form factor is calculated from simulations and compared to experimental ones.

**10. As far as I have understood, the form factor is simply a Fourier transform of electron density. I have some quick and dirty scripts to calculate those in the NMRLipids III repository:**

<https://github.com/NMRLipids/NmrLipidsCholXray/blob/master/scratch/FFactor/FFstructCALC.sh>

<https://github.com/NMRLipids/NmrLipidsCholXray/tree/master/scratch/FFactor>

**However, I have not been able to install the SIMtoEXP program (<http://link.springer.com/article/10.1007%2Fs00232-010-9254-5>) so I have not been able to check my script against the standard method. This should be straightforward issue and should become clear once I check the details. Anyway, any kind of information from full explanation with citations to the hints of relevant literature are helpful here. The more detailed discussion can be found at:** <https://github.com/NMRLipids/NMRLipids-V-Review/issues/3>

How accurate are the calculated form factors from simulations.

**11. I think that from statistical point of view accuracy is quite high, however I am not sure about the effect of undulations etc. Any kind of information from full explanation with citations to the hints of relevant literature are helpful here. The more detailed discussion can be found at:** <https://github.com/NMRLipids/NMRLipids-V-Review/issues/4>

What can be learned about the structure when comparing the form factors between experiments and simulations

**12. I have thought that if the form factor is reproduced by the simulation, the electron density profile should be reasonable. However, since some people are tuning the peak highs for better agreement, I am not sure. There is also some connection to the thickness. There is already some discussion about this in the blog with Peter Heftberger and Georg Pabst. Any kind of information from full explanation with citations to the hints of relevant literature are helpful here. The more detailed discussion can be found at:** <https://github.com/NMRLipids/NMRLipids-V-Review/issues/5>

## CONCLUSIONS

---

\* samuli.ollila@aalto.fi

- [1] A. Abragam, *The Principles of Nuclear Magnetism* (Oxford University Press, 1961).
- [2] J. Chowdhary, E. Harder, P. E. M. Lopes, L. Huang, A. D. MacKerell, and B. Roux, *J. Phys. Chem. B* **117**, 9142 (2013).
- [3] P. Prakash and R. Sankararamakrishnan, *J. Comp. Chem.* **31**, 266 (2010).
- [4] J. Seelig, *Q. Rev. Biophys.* **10**, 353 (1977).
- [5] M. Hong, K. Schmidt-Rohr, and A. Pines, *J. Am. Chem. Soc.* **117**, 3310 (1995).
- [6] J. D. Gross, D. E. Warschawski, and R. G. Griffin, *J. Am. Chem. Soc.* **119**, 796 (1997).
- [7] S. V. Dvinskikh, V. Castro, and D. Sandstrom, *Phys. Chem. Chem. Phys.* **7**, 607 (2005).
- [8] T. M. Ferreira, F. Coreta-Gomes, O. H. S. Ollila, M. J. Moreno, W. L. C. Vaz, and D. Topgaard, *Phys. Chem. Chem. Phys.* **15**, 1976 (2013).
- [9] M. Hong, K. Schmidt-Rohr, and D. Nanz, *Biophys. J.* **69**, 1939 (1995).
- [10] T. M. Ferreira, O. H. S. Ollila, R. Pigliapochi, A. P. Dabkowska, and D. Topgaard, *J. Chem. Phys.* **142**, 044905 (2015), URL <http://scitation.aip.org/content/aip/journal/jcp/142/4/10.1063/1.4906274>.
- [11] A. Botan, F. Fernando, J. F. Patrick Franois, M. Javanainen, M. Kanduc, W. Kulig, A. Lamberg, C. Loison, A. P. Lyubartsev, M. S. Miettinen, et al., *The Journal of Physical Chemistry B* **0**, null (0), PMID: 26509669, <http://dx.doi.org/10.1021/acs.jpcc.5b04878>, URL <http://dx.doi.org/10.1021/acs.jpcc.5b04878>.
- [12] D. Warschawski and P. Devaux, *Eur. Biophys. J.* **34**, 987 (2005), ISSN 0175-7571.
- [13] H. U. Gally, W. Niederberger, and J. Seelig, *Biochemistry* **14**, 3647 (1975).
- [14] H. Akutsu and J. Seelig, *Biochemistry* **20**, 7366 (1981).
- [15] B. Bechinger and J. Seelig, *Chem. Phys. Lipids* **58**, 1 (1991).
- [16] O. Berger, O. Edholm, and F. Jähnig, *Biophys. J.* **72**, 2002 (1997).
- [17] C.-J. Högberg, A. M. Nikitin, and A. P. Lyubartsev, *J. Comput. Chem.* **29**, 2359 (2008).
- [18] D. Poger, W. F. Van Gunsteren, and A. E. Mark, *J. Comput. Chem.* **31**, 1117 (2010).
- [19] J. P. Ulmschneider and M. B. Ulmschneider, *J. Chem. Theory Comput.* **5**, 1803 (2009).
- [20] A. Kukol, *J. Chem. Theory Comput.* **5**, 615 (2009).
- [21] S.-W. Chiu, S. A. Pandit, H. L. Scott, and E. Jakobsson, *J. Phys. Chem. B* **113**, 2748 (2009).
- [22] J. B. Klauda, R. M. Venable, J. A. Freites, J. W. O'Connor, D. J. Tobias, C. Mondragon-Ramirez, I. Vorobyov, A. D. M. Jr, and R. W. Pastor, *J. Phys. Chem. B* **114**, 7830 (2010).
- [23] C. J. Dickson, L. Rosso, R. M. Betz, R. C. Walker, and I. R. Gould, *Soft Matter* **8**, 9617 (2012).
- [24] J. P. M. Jämbeck and A. P. Lyubartsev, *J. Phys. Chem. B* **116**, 3164 (2012).
- [25] A. Maciejewski, M. Pasenkiewicz-Gierula, O. Cramariuc, I. Vattulainen, and T. Rog, *J. Phys. Chem. B* **118**, 4571 (2014).
- [26] R. Tjörnhammar and O. Edholm, *J. Chem. Theory Comput.* **10**, 5706 (2014).
- [27] C. J. Dickson, B. D. Madej, A. Skjevik, R. M. Betz, K. Teigen, I. R. Gould, and R. C. Walker, *J. Chem. Theory Comput.* **10**, 865 (2014).
- [28] S. Lee, A. Tran, M. Allsopp, J. B. Lim, J. Henin, and J. B. Klauda, *J. Phys. Chem. B* **118**, 547 (2014).
- [29] J. Seelig and N. Waespe-Sarcevic, *Biochemistry* **17**, 3310 (1978).
- [30] B. Perly, I. C. P. Smith, and H. C. Jarrell, *Biochemistry* **24**, 1055 (1985).
- [31] S. V. Dvinskikh, V. Castro, and D. Sandstrom, *Phys. Chem. Chem. Phys.* **7**, 3255 (2005).
- [32] A. Ulrich and A. Watts, *Biophys. J.* **66**, 1441 (1994).
- [33] H. U. Gally, G. Pluschke, P. Overath, and J. Seelig, *Biochemistry* **20**, 1826 (1981).
- [34] F. Aussenac, M. Laguerre, J.-M. Schmitter, and E. J. Dufourc, *Langmuir* **19**, 10468 (2003).
- [35] C. Altenbach and J. Seelig, *Biochemistry* **23**, 3913 (1984).
- [36] J. Seelig, P. M. MacDonald, and P. G. Scherer, *Biochemistry* **26**, 7535 (1987).
- [37] A. K. Engel and D. Cowburn, *FEBS Letters* **126**, 169 (1981).
- [38] A. Seelig and J. Seelig, *Biochemistry* **16**, 45 (1977).
- [39] A. Leftin and M. F. Brown, *Biochim. Biophys. Acta - Biomembranes* **1808**, 818 (2011).
- [40] A. Leftin, T. Molugu, C. Job, K. Beyer, and M. Brown, *Biophysical Journal* **107**, 2274 (2014).
- [41] G. Raffard, S. Steinbrückner, A. Arnold, J. H. Davis, and E. J. Dufourc, *Langmuir* **16**, 7655 (2000).
- [42] C. R. Sanders and J. P. Schwonek, *Biochemistry* **31**, 8898 (1992).
- [43] D. Marsh, *Handbook of Lipid Bilayers, Second Edition* (RSC press, 2013).
- [44] K. Mallikarjuniah, A. Leftin, J. J. Kinnun, M. J. Justice, A. L. Rogozza, H. I. Petrache, and M. F. Brown, *Biophysical Journal* **100**, 98 (2011), ISSN 0006-3495, URL <http://www.sciencedirect.com/science/article/pii/S0006349510013792>.
- [45] A. Catte, M. Giryach, M. Javanainen, M. S. Miettinen, L. Monticelli, J. Määttä, V. S. Oganessian, and O. H. S. Ollila, *The electrometer concept and binding of cations to phospholipid bilayers* (2015), DOI: 10.5281/zenodo.32175.
- [46] M. Roux, J. M. Neumann, R. S. Hodges, P. F. Devaux, and M. Bloom, *Biochemistry* **28**, 2313 (1989).
- [47] E. Kuchinka and J. Seelig, *Biochemistry* **28**, 4216 (1989).
- [48] S. Ollila, M. T. Hyvönen, and I. Vattulainen, *J. Phys. Chem. B* **111**, 3139 (2007).
- [49] L. Vermeer, B. de Groot, V. Rat, A. Milon, and J. Czaplicki, *Eur. Biophys. J.* **36**, 919 (2007), ISSN 0175-7571, URL <http://dx.doi.org/10.1007/s00249-007-0192-9>.
- [50] D. Poger and A. E. Mark, *J. Chem. Theory Comput.* **8**, 4807 (2012).
- [51] M. Bachar, P. Brunelle, D. P. Tieleman, and A. Rauk, *J. Phys. Chem. B* **108**, 7170 (2004).
- [52] J. Wong-ekkabut, Z. Xu, W. Triampo, I.-M. Tang, D. P. Tieleman, and L. Monticelli, *Biophysical Journal* **93**, 4225 (2007), ISSN 0006-3495, URL <http://www.sciencedirect.com/science/article/pii/S0006349507716752>.
- [53] A. Vogel and S. Feller, *The Journal of Membrane Biology* **245**, 23 (2012), ISSN 0022-2631.
- [54] P. van der Ploeg and H. J. C. Berendsen, *The Journal of Chemical Physics* **76** (1982).
- [55] E. Egberts and H. J. C. Berendsen, *J. Chem. Phys.* **89**, 3718 (1988).

- [56] T. R. Stouch, *Molecular Simulation* **10**, 335 (1993).
- [57] E. Egberts, S.-J. Marrink, and H. Berendsen, *European Biophysics Journal* **22**, 423 (1994), ISSN 0175-7571, URL <http://dx.doi.org/10.1007/BF00180163>.
- [58] J. W. Essex, M. M. Hann, and W. G. Richards, *Philos. T. Roy. Soc. B* **344**, 239 (1994).
- [59] A. Robinson, W. Richards, P. Thomas, and M. Hann, *Biophys. J.* **67**, 2345 (1994).
- [60] M. T. Hyvönen, M. Ala-Korpela, J. Vaara, T. T. Rantala, and J. Jokisaari, *Chem. Phys. Lett.* **246**, 300 (1995).
- [61] V. Kothekar, *Ind. J. Biochem. Biophys.* **33**, 431 (1996).
- [62] D. P. Tieleman and H. J. C. Berendsen, *J. Chem. Phys.* **105**, 4871 (1996).
- [63] W. Shinoda, N. Namiki, and S. Okazaki, *J. Chem. Phys.* **106**, 5731 (1997).
- [64] D. P. Tieleman, S. J. Marrink, and H. J. C. Berendsen, *Biochim. Biophys. Acta* **1331**, 235 (1997).
- [65] M. Lafleur, P. Cullis, and M. Bloom, *European Biophysics Journal* **19**, 55 (1990), ISSN 0175-7571, URL <http://dx.doi.org/10.1007/BF00185086>.
- [66] J. A. Urbina, S. Pekerar, H. biao Le, J. Patterson, B. Montez, and E. Oldfield, *Biochimica et Biophysica Acta (BBA) - Biomembranes* **1238**, 163 (1995), ISSN 0005-2736, URL <http://www.sciencedirect.com/science/article/pii/S000527369500117L>.
- [67] R. J. Mashl, H. L. Scott, S. Subramaniam, and E. Jakobsson, *Biophys. J.* **81**, 3005 (2001).
- [68] C.-J. Hgberg, , and A. P. Lyubartsev\*, *The Journal of Physical Chemistry B* **110**, 14326 (2006).
- [69] Q. Zhu, K. H. Cheng, and M. W. Vaughn, *J. Phys. Chem. B* **111**, 11021 (2007).
- [70] J. B. Lim, B. Rogaski, and J. B. Klauda, *J. Phys. Chem. B* **116**, 203 (2012).
- [71] J. P. M. Jambeck and A. P. Lyubartsev, *Phys. Chem. Chem. Phys.* **15**, 4677 (2013).
- [72] B. D. Madej, I. R. Gould, and R. C. Walker, *The Journal of Physical Chemistry B* **119**, 12424 (2015).
- [73] M. Hölte, T. Förster, B. Brandt, T. Engels, W. von Rybinski, and H.-D. Hölte, *Biochim. Biophys. Acta* **1511**, 156 (2001).
- [74] M. T. Hyvönen, T. T. Rantala, and M. Ala-Korpela, *Biophys. J.* **73**, 2907 (1997).
- [75] M. Hyvnen, M. Ala-Korpela, J. Vaara, T. T. Rantala, and J. Jokisaari, *Chemical Physics Letters* **268**, 55 (1997), ISSN 0009-2614, URL <http://www.sciencedirect.com/science/article/pii/S0009261497001711>.
- [76] M. T. Hyvönen and P. T. Kovanen, *Eur. Biophys. J.* **34**, 294 (2005).
- [77] W. Kulig, M. Pasenkiewicz-Gierula, and T. Róg, *Chem. Phys. Lipids* pp. *In Press, Accepted Manuscript*, <http://dx.doi.org/10.1016/j.chemphyslip.2015.07.002> (2015), URL <http://www.sciencedirect.com/science/article/pii/S0009308415300074>.
- [78] J. Kapla, B. Stevansson, M. Dahlberg, and A. Maliniak, *J. Phys. Chem. B* **116**, 244 (2012).
- [79] G. Lipari and A. Szabo, *J. Am. Chem. Soc.* **104**, 4546 (1982).
- [80] A. Nowacka, P. C. Mohr, J. Norrman, R. W. Martin, and D. Topgaard, *Langmuir* **26**, 16848 (2010).
- [81] M. F. Roberts, A. G. Redfield, and U. Mohanty, *Biophys. J.* **97**, 132 (2009).
- [82] E. Lindahl and O. Edholm, *J. Chem. Phys.* **115**, 4938 (2001).
- [83] J. B. Klauda, R. M. Venable, A. D. M. Jr., and R. W. Pastor, in *Computational Modeling of Membrane Bilayers*, edited by S. E. Feller (Academic Press, 2008), vol. 60 of *Current Topics in Membranes*, pp. 1 – 48.
- [84] J. Wohlt, W. K. den Otter, O. Edholm, and W. J. Briels, *J. Chem. Phys.* **124**, 154905 (2006).
- [85] P. G. Scherer and J. Seelig, *Biochemistry* **28**, 7720 (1989).
- [86] These changes were later shown to be consistent with the addition of different charges into the bilayer, and the electrometer concept was introduced to measure the amount of charge incorporated in the bilayer interface [85].
- [87] This increase is related to the P-N vector tilting more parallel to the membrane plane [11] which is in agreement with electrometer concept suggesting that penetrating charge has opposite effect on headgroup tilt leading to decrease of order parameters [45, 85].
- [88] In this work CH<sub>2</sub>/CH<sub>3</sub> groups in cholesterol were changed to LP<sub>2</sub>/LP<sub>3</sub> groups to make it more consistent with the Berger parameters. This is not usually done in the studies done with these model.

## ToDo

	P.
1. Samuli: Add citations to the introduction. Rewriting is also needed . . . . .	1
2. This is the first sketch of this section. It is composed from the content in the blog and from the things which came into my mind. A lot of references should be added, the text should polished, things should be added and checked and figures should be improved. However, the main strucutre and idea of the section should be visible. . . . .	2
3. How accurate exactly? . . . . .	3
4. Maybe specify to which ones? . . . . .	3
5. Has this been done for the C <sub>2</sub> carbon in the <i>sn</i> -2 chain? . . . . .	6
6. The analysis with ions not actually done yet! . . . . .	9
7. This is quite straightforward to write for me and there is quite good support from our recent work [10]. I will write the first version as soon as I can. . . . .	11
8. Which is the experimental quantity that the scattering machinery exactly puts out? How the form factor is determined from the experimental observables?	

Which assumptions are needed here?

There is already some discussion about this in the blog by Peter Heftberger and Georg Pabst, but any kind of information from full explanation with citations to the hints of relevant literature are helpful here. The more detailed discussion can be found at: [https://github.com/NMRLipids/NMRLipids\\_V-Review/issues/1](https://github.com/NMRLipids/NMRLipids_V-Review/issues/1) . . . . . 15

9. Has this been discussed in the literature already? Any kind of information from full explanation with citations to the hints of relevant literature are helpful here. The more detailed discussion can be found at: [https://github.com/NMRLipids/NMRLipids\\_V-Review/issues/2](https://github.com/NMRLipids/NMRLipids_V-Review/issues/2) . . . . . 15

10. As far as I have understood, the form factor is simply a Fourier transform of electron density. I have some quick and dirty scripts to calculate those in the NMRLipids III repository: <https://github.com/NMRLipids/NmrLipidsCholXray/blob/master/scratch/FFactor/FFstructCALC.sh>  
<https://github.com/NMRLipids/NmrLipidsCholXray/tree/master/scratch/FFactor>

However, I have not been able to install the SIMtoEXP program (<http://link.springer.com/article/10.1007%2Fs00232-0>)

so I have not been able to check my script against the standard method. This should be straightforward issue and should become clear once I check the details. Anyway, any kind of information from full explanation with citations to the hints of relevant literature are helpful here. The more detailed discussion can be found at: [https://github.com/NMRLipids/NMRLipids\\_V-Review/issues/3](https://github.com/NMRLipids/NMRLipids_V-Review/issues/3) . . . . . 15

11. I think that from statistical point of view accuracy is quite high, however I am not sure about the effect of undulations etc. Any kind of information from full explanation with citations to the hints of relevant literature are helpful here. The more detailed discussion can be found at: [https://github.com/NMRLipids/NMRLipids\\_V-Review/issues/4](https://github.com/NMRLipids/NMRLipids_V-Review/issues/4) . . . . . 15

12. I have thought that if the form factor is reproduced by the simulation, the electron density profile should be reasonable. However, since some people are tuning the peak highs for better agreement, I am not sure. There is also some connection to the thickness. There is already some discussion about this in the blog with Peter Heftberger and Georg Pabst. Any kind of information from full explanation with citations to the hints of relevant literature are helpful here. The more detailed discussion can be found at: [https://github.com/NMRLipids/NMRLipids\\_V-Review/issues/5](https://github.com/NMRLipids/NMRLipids_V-Review/issues/5) . . . . . 15